Recyclability Study on Inconel 718 and Ti-6Al-4V Powders for Use in Electron Beam Melting

PEEYUSH NANDWANA, WILLIAM H. PETER, RYAN R. DEHOFF, LARRY E. LOWE, MICHAEL M. KIRKA, FRANCISCO MEDINA, and SUDARSANAM S. BABU

Powder bed-based additive manufacturing technologies offer a big advantage in terms of reusability of the powders over multiple cycles that result in cost savings. However, currently there are no standards to determine the factors that govern the powder reuse times. This work presents the results from a recyclability study conducted on Inconel 718 and Ti-6Al-4V powders. It has been found that the Inconel 718 powders are chemically stable over a large number of cycles and their reuse time is limited by physical characteristics of powders such as flowability. Ti-6Al-4V, on the other hand, finds its reuse time governed by the oxygen pick up that occurs during and in between build cycles. The detailed results have been presented.

DOI: 10.1007/s11663-015-0477-9
© The Minerals, Metals & Materials Society and ASM International 2015

I. INTRODUCTION

POWDER bed-based additive manufacturing (AM) technologies like selective laser melting (SLM) and electron beam melting (EBM) provide users the ability to melt selective areas on a uniform powder bed layer by layer to create a part using a computer aided design (CAD) model. These technologies offer advantages over conventional manufacturing technologies in terms of ease of fabrication of complex parts, reduced process steps, and potential cost savings including reduction of machining compared to conventional fabrication techniques such as casting.[1–3] In order to realize these advantages, the supply chain and reliable feedstock parameters must be established for use with the equipment. The feedstock properties such as chemistry, size distribution, porosity, flowability, and apparent density play an important role in determining the surface finish, mechanical properties, chemistry, and consistency of the fabricated parts. The cost affordability of these AM techniques also relies on the usage of recycled powders to produce parts with consistent chemistries. The high-cost powders for specialty applications like aerospace and biomedical applications make the powder reuse times a key component in governing their affordability. There has been an increased research interest in fabricating parts using EBM system commercialized by Arcam AB, Sweden. However, most studies have focused on process control, microstructural evolution, and subsequent mechanical properties. Columnar grains along the build direction is a typical microstructural feature of electron-beam fabricated samples and research is ongoing to control process parameters to break down the columnar microstructure into a more equiaxed microstructure.[1,4,5] There have been limited papers discussing the role of feedstock material in determining the final material properties.[6] In a typical production setup, powders are changed often to maintain the chemistry of the builds as well as to maintain the flowability of the powders themselves. It has been estimated that, in a given batch for selective laser sintering, not more than 67 pct of the powders should be from the recycled batch.[7] There is a need for systematic recyclability studies to demonstrate the stability of the powders for use over extended time periods as well as the relation between the powder and the build chemistries for multiple powders and chemistries. The present study compares the influence of powder reuse times for two alloys of high interest, Inconel 718 and Ti-6Al-4V powders, in the EBM process and highlights the differences in the two alloy powders in terms of the changes that occur as a result of reuse under the worst-case scenario.

II. EXPERIMENTAL

Inconel 718 powders procured from Raymor Inc. and Ti-6Al-4V powders obtained from Arcam AB were used for the current study that was carried out on the Arcam A^2

PEEYUSH NANDWANA, Postdoctoral Fellow, Deposition Science and Technology Group, RYAN R. DEHOFF, Group Leader, Deposition Science and Technology Group, LARRY E. LOWE, Staff Technician, and MICHAEL M. KIRKA, Staff Scientist, Deposition Science and Technology Group, are with the Manufacturing Demonstration Facility, Oak Ridge National Laboratory, Oak Ridge, TN, and also with the Materials Science and Technology Division, Oak Ridge National Laboratory, Oak Ridge, TN. Contact e-mail: nandwanap@ornl.gov WILLIAM H. PETER, Deputy Director, Manufacturing Demonstration Facility, is with the Manufacturing Demonstration Facility, Oak Ridge National Laboratory, and also with the Energy and Transportation Science Division, Oak Ridge National Laboratory, Oak Ridge, TN. FRANCISCO MEDINA, Senior Specialist in Materials Development Group, is with Arcam AB, Mölndal, Sweden. SUDARSANAM S. BABU, Governor's Chair, is with the Manufacturing Demonstration Facility, Oak Ridge National Laboratory, and with the Energy and Transportation Sciences Division, Oak Ridge National Laboratory, and also with the Department of Mechanical, Aerospace and Biomedical Engineering, The University of Tennessee, Knoxville, TN.
Manuscript submitted August 4, 2015.

Published online: 20 October 2015

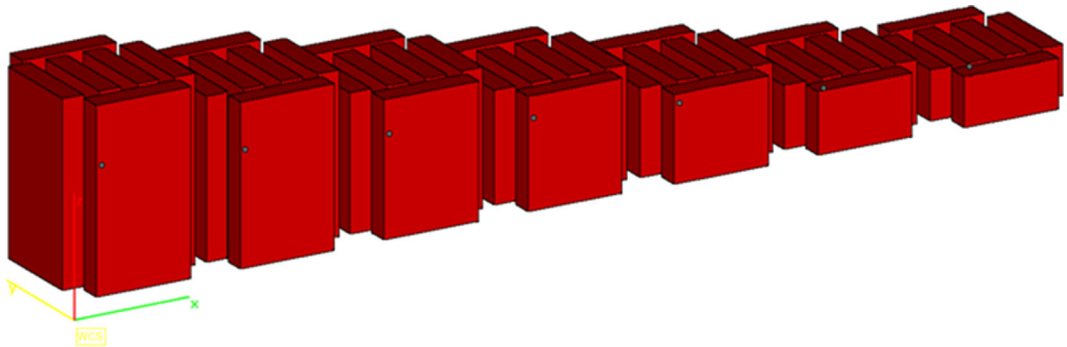

Fig. 1—Schematic of the build design for the recyclability study.

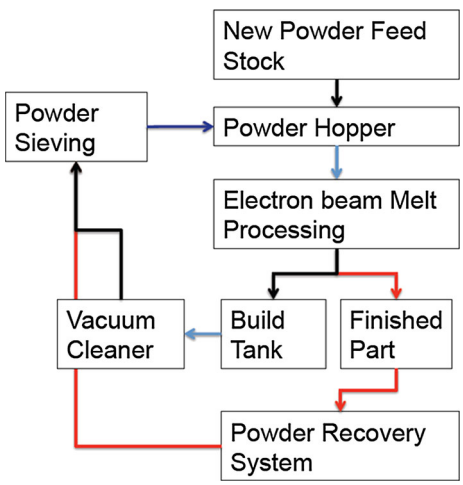

Fig. 2—Schematic of powder cycle during the recyclability study.

electron beam melter developed by Arcam AB in Sweden. The nominal powder size distribution varied from 45 to 105 μm and 100 kgs of powder was used in the beginning of the study. Six builds were fabricated for the Inconel 718 alloy and five builds were fabricated for Ti-6Al-4V alloy. The build dimensions were designed such that at the end of each build the powder hoppers would completely run out of powder, thus exposing all the powder to the electron beam. This experiment was designed to understand the worst-case scenario since keeping the build heights constant would have required fresh powders to be added after every build and would have made it difficult to determine the changes in chemistry and physical properties of the bulk powders due to electron beam interaction. Figure 1 shows the build geometries that were fabricated for the present study. After each build, the powders were vacuumed out of the build chamber and the fabricated part was blasted in the powder recovery system (PRS) to recover the partially sintered powders. The powders recovered were then mixed with the vacuumed powders and then were sieved on a vibratory sieve with a 100-mesh (150 μm) screen. Powders greater than 150 μm were discarded. A sample was collected from these mixed powders for analysis before loading these powders in the hopper and the powder bed to prepare the Arcam for the next build. Figure 2 shows a schematic of the process employed to conduct this study. Also, some samples were collected from the partially sintered layer to understand if there are local chemistry changes in the powder that encloses the build as compared to the bulk powders. The chemical analyses for Inconel 718 were carried out in accordance with ASTM standards ASTM E 1019-11, ASTM E 1447-09, and ASTM E 1097-12. The analyses for Ti-6Al-4V were carried out in accordance with ASTM standards ASTM E1409-13, ASTM E 1941-10, ASTM E 1447-09, and ASTM E 2371-13. During the fabrication of builds, metallization, due to evaporation of low vaporization elements with higher vapor pressure, was observed on the heat shields. The metallized layer was removed from the heat shield for chemistry analysis. The collected powder samples, metallized layer, and builds were then subjected for chemistry analysis. The powder samples were also analyzed for flow characteristics using a Hall flow meter in compliance with ASTM standard ASTM B213-03.[8] Powder size distribution analysis was carried out on a Horiba LA-950 Laser Diffraction Particle Analyzer that meets or exceeds the ISO 13320 requirements. Scanning electron microscopy (SEM) and energy-dispersive spectroscopy (EDS) were carried out on the powder samples and the metallized layer using a Hitachi S3400 environmental microscope. Overall, the Inconel 718 powders were subjected to about 267 hours of build time and Ti-6Al-4V powders were subjected to about 175 hours of build time.

III. RESULTS AND DISCUSSION

A. *Recyclability Study on Inconel 718*

Table I presents the chemical composition of as-received powders, and powders after the Build Cycles 1 and 6. It can be observed that the chemical compositions of powders after the Build Cycles 1 and 6 are practically unchanged compared to those of as-received powders and are within the limits of experimental errors. There is a slight increase in oxygen concentration from 0.014 to 0.023 wt pct after six build cycles. Table II, on the other hand presents the chemistries of powder samples collected from different locations of the build table in order to evaluate the local changes in powder chemistry, if any. It can be seen that the powder chemistries for powder samples taken from different locations after Build 6 are the same as the average powder chemistry

Table I. Powder Chemistries for Inconel 718 Powders After Different Build Cycles

	As-received Powder	Powders After Build 1	Powders After Build 6
Carbon	0.044	0.043	0.042
Sulfur	0.002	0.002	0.001
Oxygen	0.014	0.014	0.022
Nitrogen	0.020	0.019	0.020
Hydrogen	0.0002	0.0002	0.0002
Nickel	53.03	52.75	53.60
Chromium	18.40	18.36	18.09
Molybdenum	3.10	3.08	2.96
Niobium	4.86	4.95	4.84
Manganese	0.095	0.096	0.088
Copper	0.15	0.16	0.14
Aluminum	0.43	0.41	0.42
Titanium	0.89	0.91	0.86
Silicon	0.19	0.23	0.20
Phosphorous	0.006	0.009	0.0083
Boron	<0.0005	<0.0005	0.0013
Cobalt	0.14	0.16	0.13
Iron	18.59	18.80	18.57

Table II. Comparison in Powder Chemistries for Powder at Different Locations After Build 6

	Partially Sintered Powder From Bottom of Build 6	Partially Sintered Powder From Top of Build 6	Powders After Build 6
Carbon	0.043	0.042	0.042
Sulfur	0.001	0.001	0.001
Oxygen	0.021	0.023	0.022
Nitrogen	0.020	0.020	0.020
Hydrogen	0.0002	0.0002	0.0002
Nickel	53.79	53.12	53.60
Chromium	17.87	18.09	18.09
Molybdenum	3.05	3.16	2.96
Niobium	4.80	4.79	4.84
Manganese	0.088	0.088	0.088
Copper	0.14	0.14	0.14
Aluminum	0.42	0.42	0.42
Titanium	0.87	0.89	0.86
Silicon	0.20	0.20	0.20
Phosphorous	0.0065	0.0083	0.0083
Boron	0.0010	0.0012	0.0013
Cobalt	0.13	0.13	0.13
Iron	18.84	18.87	18.57

Table III. Build Chemistries for Builds 1 and 6 Compared with the Chemistry of As-Received Powders

	As-received Powder	Chemistry of Build 1	Chemistry of Build 6
Carbon	0.044	0.044	0.040
Sulfur	0.002	0.002	0.002
Oxygen	0.014	0.006	0.009
Nitrogen	0.020	0.016	0.015
Hydrogen	0.0002	0.0005	0.0003
Nickel	53.03	53.33	53.27
Chromium	18.40	17.84	18.15
Molybdenum	3.10	3.13	3.15
Niobium	4.86	4.96	4.97
Manganese	0.095	0.080	0.073
Copper	0.15	0.13	0.13
Aluminum	0.43	0.44	0.44
Titanium	0.89	0.91	0.91
Silicon	0.19	0.22	0.23
Phosphorous	0.006	0.008	0.008
Boron	<0.0005	<0.0005	<0.0005
Cobalt	0.14	0.15	0.15
Iron	18.59	18.70	18.42

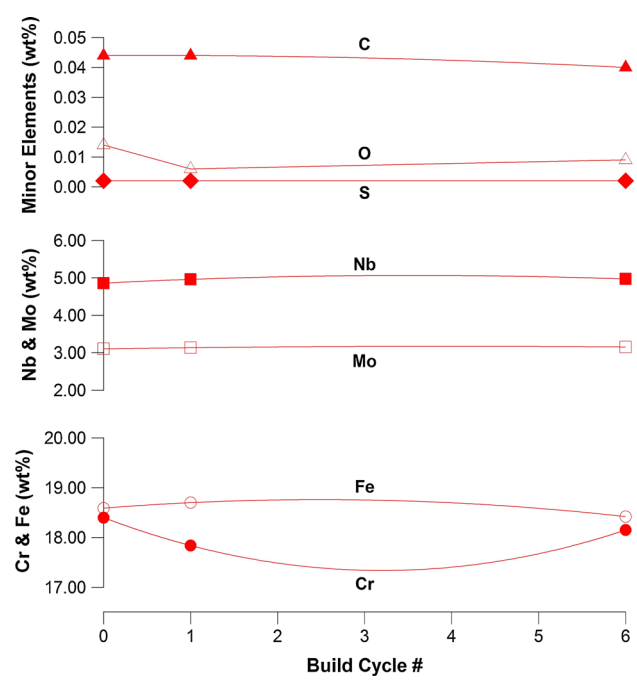

Fig. 3—Change in composition of Inconel 718 builds after each build cycle.

and that of as-received powders. Thus, there are no local changes in powder chemistry resulting from partial sintering of powders during the fabrication of the build. Table III presents the chemistries of Builds 1 and 6 and contrasted them with the chemistry of the as-received powders. It can be seen that the build chemistries are consistent over the build cycles and similar to those of powder chemistries after subsequent build cycles. These observations are summarized in Figure 3, which shows a slight increase in the oxygen concentration in the builds after six cycles from 0.006 to 0.009-wt pct. Build 0 denotes the chemistry of the as-received powder that was used as a reference to understand the relation between powders and build chemistries. The recycled powders were analyzed for flow behavior as a function of build cycle and the observations are presented in Figure 4. No noticeable change is observed in the flowability of the powders as a function of build cycles. Scanning electron microscopy was carried out on the powders to understand the change in morphology of powders resulting from the reuse and the SEM micrographs are presented in Figure 5. The images are labeled

0 through 6 with 0 being the as-received powders and 6 being the powders after the Build 6. It can be seen from the SEM micrograph for powders after the Build Cycle 6 that there are fines that have sintered into agglomerates that could not be broken down in the PRS. However, the volume fraction of the fines does not seem to be large enough to cause any noticeable change in the flow times. Figure 6 shows the change in powder size distribution as a function of build cycles with the inset showing the change in mean powder diameter as a function of build cycles. It can be noted that there is a slight increase in the mean powder diameter and the curve shits to the right after the cycle 6, though a clear trend is not visible from the curve as a function of the build cycle. From the mean powder diameter *vs* build cycle curve presented in the inset, it can be seen that though the increase in powder size is not linear, on an average the mean powder diameter increases by the end of Build Cycle 6. This may be a consequence of the removal of loose fines as the powders are circulated through the PRS. An independent study was carried out at Arcam AB in Sweden on an Arcam A^{x} machine and it was confirmed that the build chemistries were similar to the as-received powder chemistry and remain unchanged over six build cycles. The fact that the two studies concur, affirms the fact that Inconel 718 powder is stable for use in electron beam melting-based additive manufacturing.[9]

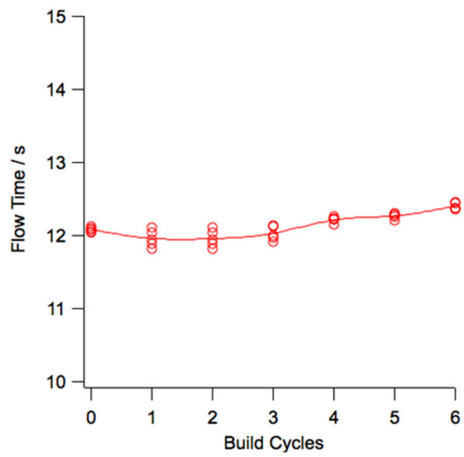

Fig. 4—Change in flowability of Inconel 718 powder with build cycles.

B. *Recyclability Study on Ti-6Al-4V*

The recyclability on Ti-6Al-4V was carried out using EIGA powders. Of the five planned builds, only the final three builds reached the programed build heights. The first two builds stopped short possibly due to arc trips and the runs were terminated. The plots henceforth show area marked as relevant data that gives a true picture of the change in powder and build chemistries.

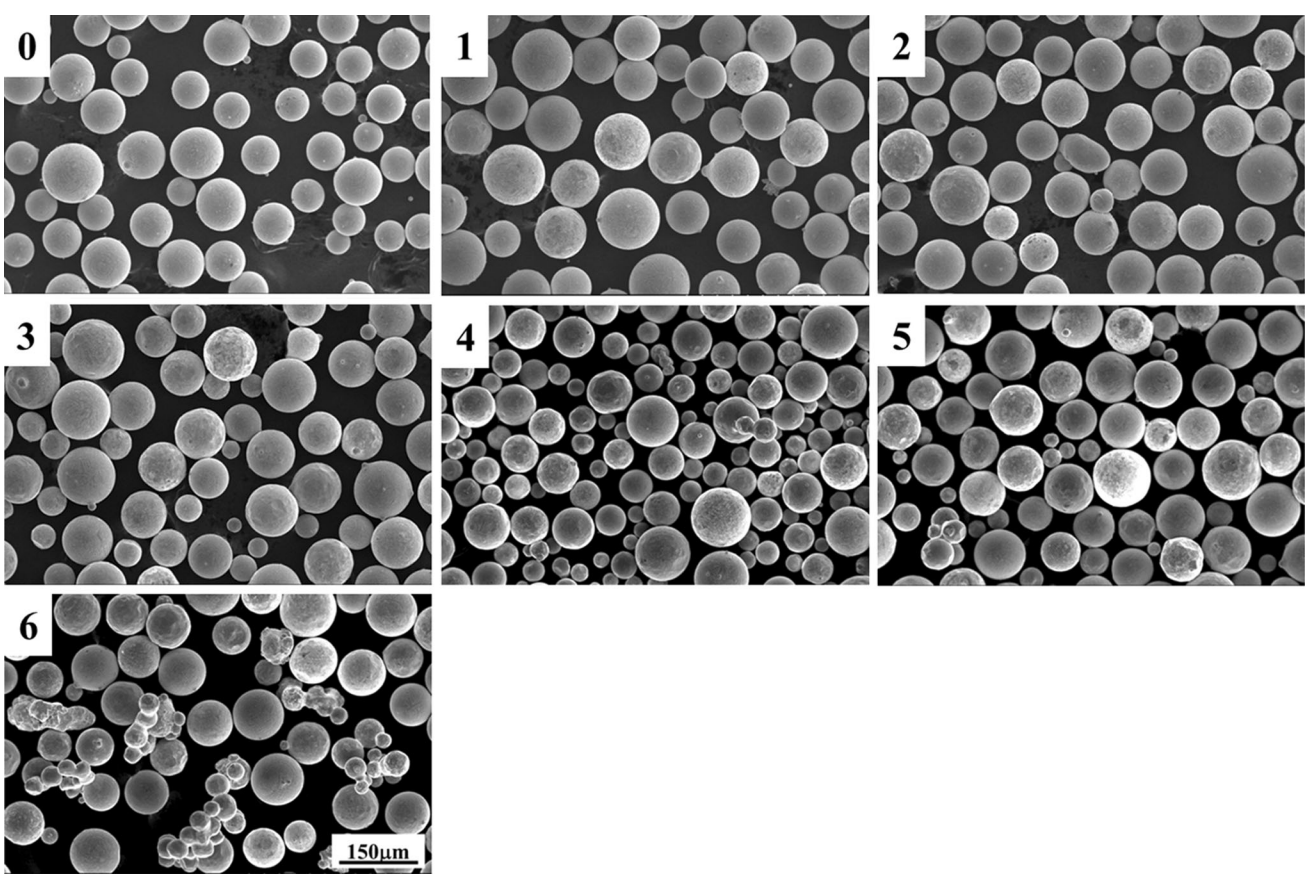

Fig. 5—Secondary electron micrographs of Inconel 718 powders after various build cycles.

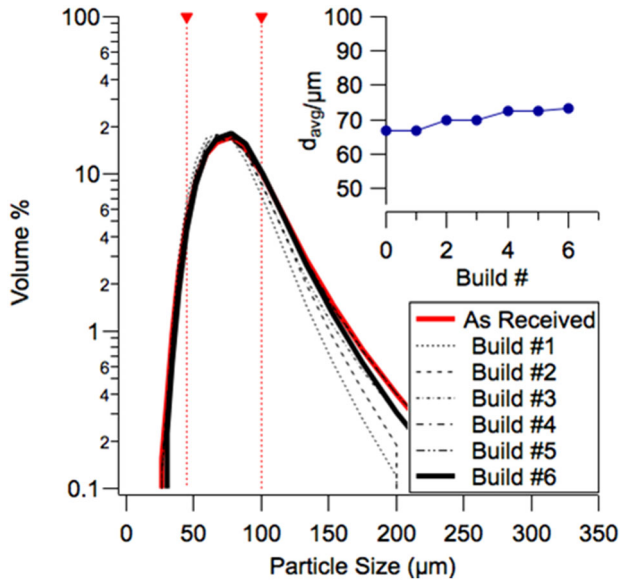

Fig. 6—Change in powder size distribution of Inconel 718 powders after different build cycles.

Table IV. Chemistries of Ti6Al4V Powders After Build 5 and Chemistries of Build 1 and Build 5 Compared to Those of As-Received Powders

	As-Received Powder	Powder After Cycle 5	Build 1	Build 5
Aluminum	6.27	6.36	5.82	6.17
Vanadium	4.14	4.39	4.23	4.35
Oxygen	0.138	0.182	0.141	0.168
Nitrogen	0.025	0.025	0.019	0.025
Carbon	0.015	0.018	0.020	0.028
Hydrogen	0.0016	0.0024	0.0025	0.0015
Iron	0.19	0.20	0.20	0.22
Niobium	N/A	<0.002	N/A	N/A
Tungsten	N/A	<0.002	N/A	N/A
Copper	N/A	N/A	0.015	0.029
Silicon	0.022	0.023	0.024	0.020

Table V. Shows the Al, V, and O Concentrations in the Builds Over 5 Build Cycles

	Build 1	Build 2	Build 3	Build 4	Build 5
Aluminum	5.82	5.86	5.68	5.80	6.17
Vanadium	4.23	4.17	4.15	4.24	4.35
Oxygen	0.141	0.145	0.156	0.163	0.168
Hydrogen	0.0025	0.0006	0.0012	0.0011	0.0015
Iron	0.20	0.20	0.20	0.20	0.22

The chemistries of the Ti-6Al-4V as-received powders, powders after Build Cycle 5 and those of Builds 1 and 5 are presented in Table IV. It can be seen that over the 175-hour exposure to the electron beam the powder chemistry does not fluctuate much but for the increase in oxygen concentration which was expected considering the affinity of titanium to pick up oxygen. However, it is interesting to note that the aluminum concentration of

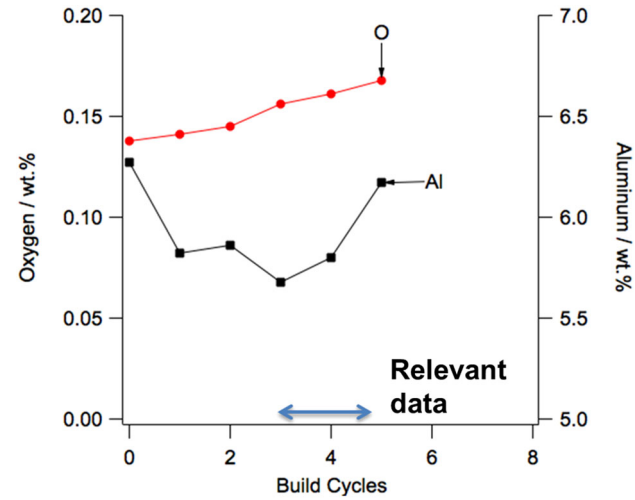

Fig. 7—Change in Al and O concentrations of Ti builds as a function of build cycle.

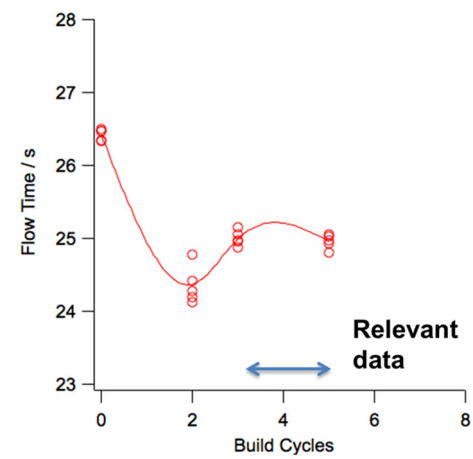

Fig. 8—Variation in flowability of Ti-6Al-4V powders with build cycles.

Build 1 is different than that of Build 5 and that Build 5 is richer in oxygen than the first one. Since aluminum and oxygen are known to have a considerable influence on the alloy properties, all five builds were analyzed for aluminum and oxygen compositions. The aluminum and oxygen concentrations steadily increased with each build cycle as presented in Table V, for Builds 3 through 5 which are the relevant builds for the current study. However, the oxygen concentration remains within the specification (<0.20 wt pct) even after five builds, which was in accordance with ASTM standard ASTM F2924-14.[10] Figure 7 shows the change in Al and O concentrations in the fabricated parts as a function of build cycle. The increase in oxygen concentration is due to the oxygen pick up during powder changing step as well as during part recovery in the PRS system. This has been investigated and presented by Tang *et al.*[6] The main source of oxygen pickup is *via* adsorption of water molecules on the powder surface as the powder is

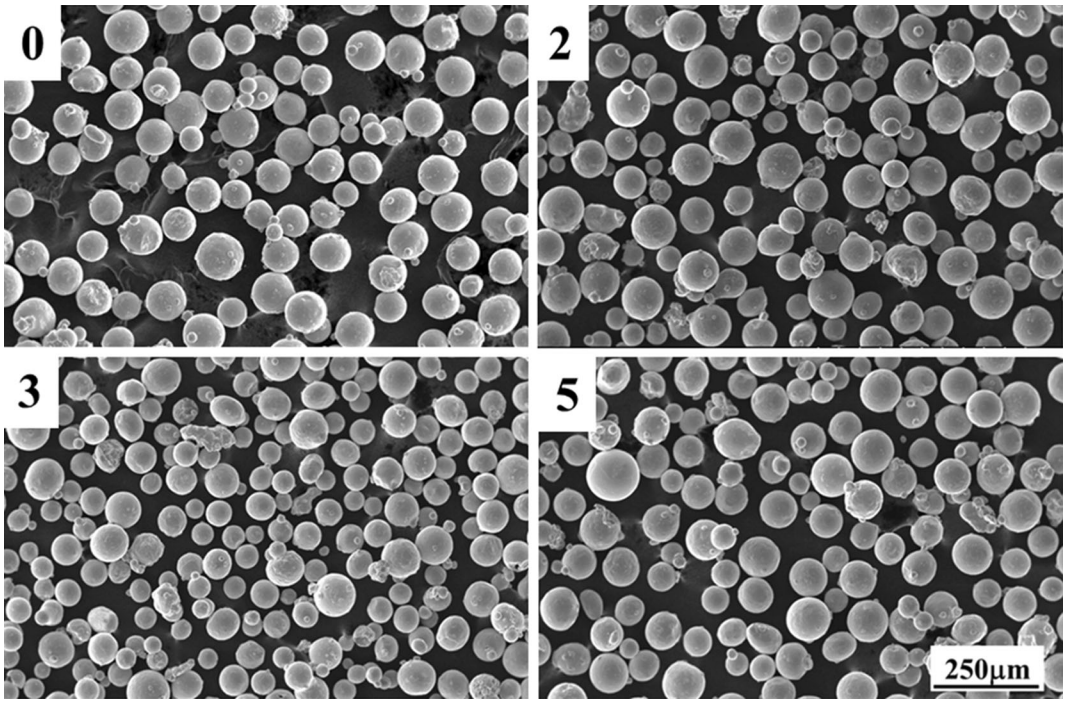

Fig. 9—Secondary electron micrographs of Ti-6Al-4V powders for as-received and after build cycles 2, 3, and 5.

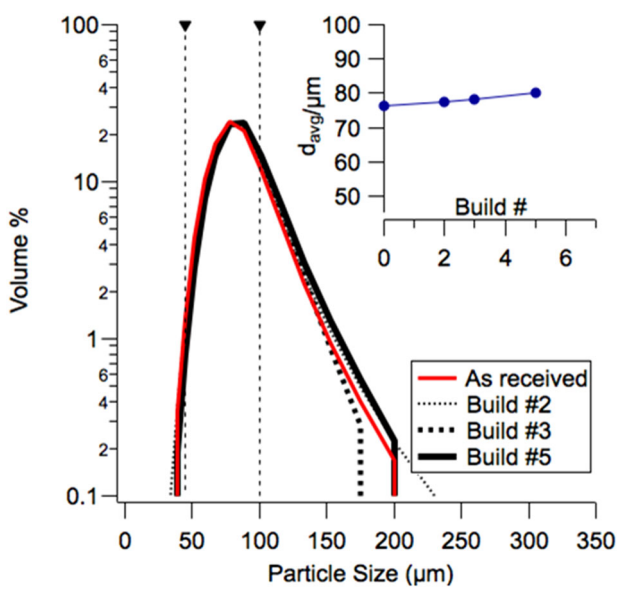

Fig. 10—Change in powder size distribution of Ti-6Al-4V powders after different build cycles.

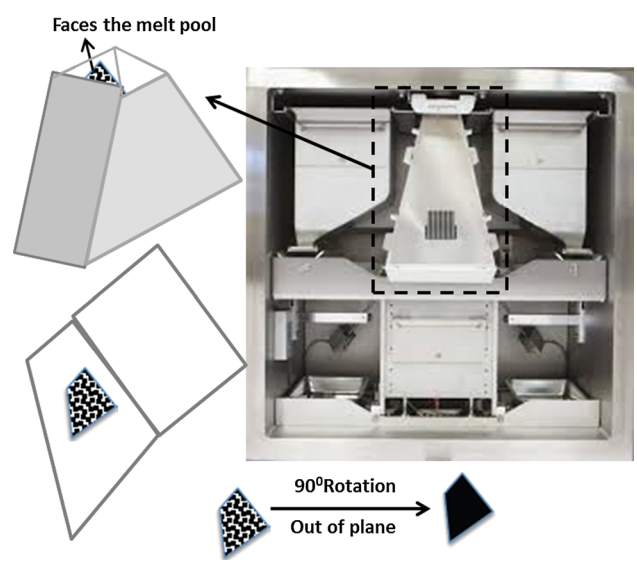

Fig. 11—Heat shield inside the Arcam system along with the schematic showing the formation of the rough and smooth sides of the metallized layers.

exposed to the atmosphere during powder change outs and in PRS. At elevated temperatures, the water molecule dissociates and the powders can pick up the oxygen. Muth *et al.* have discussed this phenomenon in detail in gas tungsten arc (GTA) welding of powder-metallurgy-produced titanium alloys.[11] After the recyclability study, the powders were subjected to flowability measurements and the flow curve is presented in Figure 8. It can be seen that there is an initial drop in the flow time, possibly due to removal of fines as the powder is subjected to PRS. However, there is no change in the flowability in the relevant area of the study that comprises builds 3, 4, and 5. Scanning electron microscopy was carried out on the powders but no significant difference emerged out in terms of sintering of fines or changes in powder morphology as seen in Figure 9. Figure 10 shows that there is no discernible change in powder size distribution as a function of build cycles. The inset shows the change in mean powder

diameter over the build cycles and there is no significant change in the average powder diameter in the relevant data for the study.

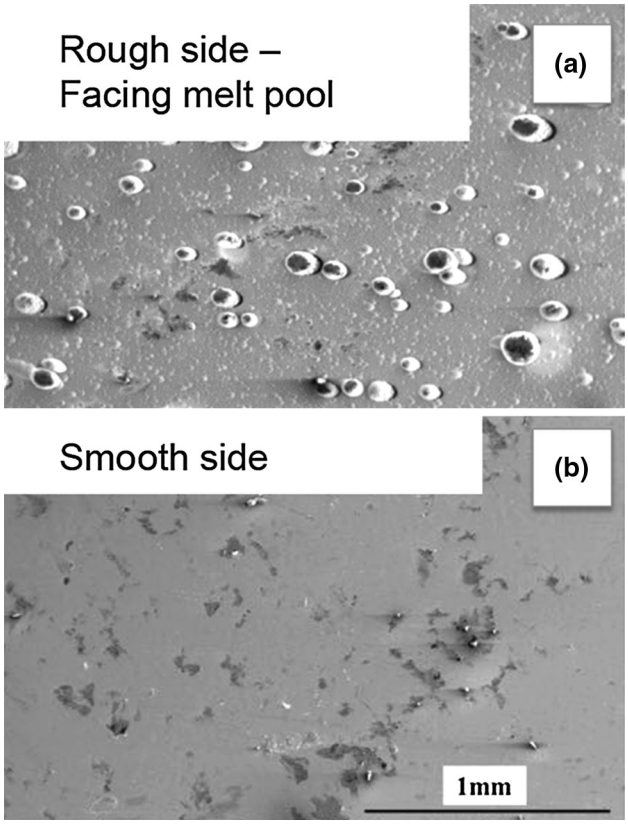

Fig. 12—Secondary electron micrograph of the rough and smooth sides of metallized layer.

C. *Metallization*

The build chamber in the Arcam consists of four heat shields, to contain the heat within the build area. As the electron beam melts the powder, multiple things can happen which are as follows: (a) small fractions of powder particles can fly off from the powder bed and impinge the heat shield as has been captured during *in situ* process monitoring, (b) some of the high vapor pressure elements can vaporize and condense on the heat shield and, (c) droplets from the melt pool can splatter and condense on the heat shield. This results in formation of a metallized layer on the heat shield during the course of a build cycle. The metallized layer, during the course of long build times, can crumple and fall off in the melt pool, thus affecting the local chemistry and hence understanding the metallized layer becomes paramount. The metallized layer was scraped off from the heat shield and consisted of rough and smooth sides with the rough side being the one facing the inside of the chamber and the melt pool. The inside of the chamber with the heat shields and the formation of rough and smooth sides are schematically shown in Figure 11. Significant metallization was observed for both Inconel 718 and Ti-6Al-4V builds. The rough and smooth sides of the metallized layers were analyzed using scanning electron microscopy and EDS. Figure 12(a) shows the rough side of the metallized layer obtained from the Inconel 718 build. It can be seen that the rough side consists of spherical particles embedded in a matrix. A similar phenomenon was observed in the case of Ti-6Al-4V builds as well. Figure 12(b) shows the secondary electron image of the smooth side of the metallized layer. EDS analysis was carried out to determine the composition of the embedded particles and matrix on the rough side as well as to determine the chemistry of the smooth side. From the plots in

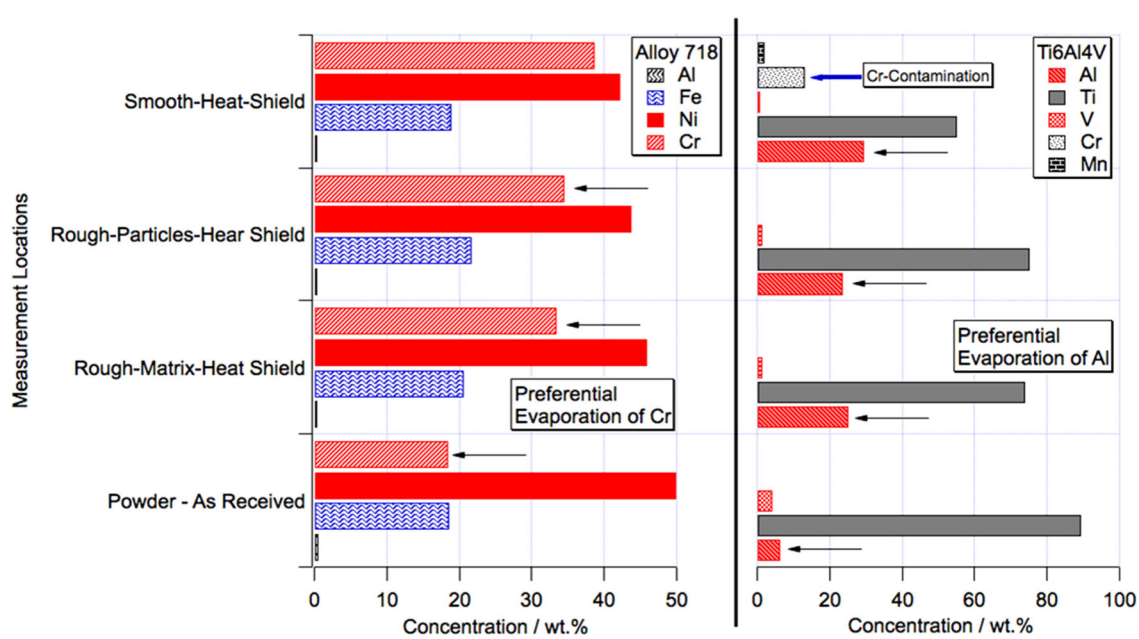

Fig. 13—Preferential evaporation of Cr and Al from Inconel 718 and Ti-6Al-4V, respectively.

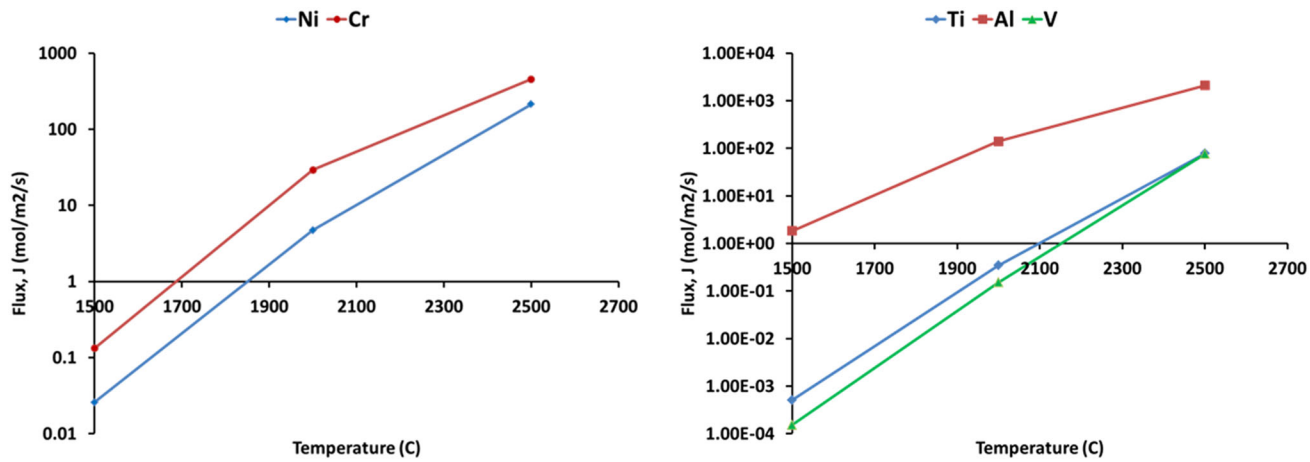

Fig. 14—Vaporization flux of relevant elements for Inconel 718 and Ti-6Al-4V alloys.

Figure 13, it can be seen that there is a preferential evaporation of chromium and aluminum from Inconel 718 and Ti-6Al-4V, respectively. Also it can be seen that the matrix and the embedded particles have similar chemical compositions. It hints toward the possible condensation of Cr- and Al-rich vapors that form the matrix phase for the two alloy systems. Analytical heat transfer calculations on Inconel 718 by Dehoff *et al.* have shown that the peak temperatures can exceed the boiling point of Inconel 718 under certain processing conditions, thereby causing preferential evaporation of high vapor pressure elements.[5] In order to get an idea of the relative rates of different elements observed on the rough side of the heat shield, a simple model employing the Langmuir equation was used. The equation is given as follows:[12]

$$J = P_o(2\pi MRT)^{-1/2},$$

where J is the vaporization flux, P_o is the equilibrium vapor pressure of the vaporizing species over the liquid, M is the molecular weight of the vaporizing species, R is the gas constant, and T is the temperature. It becomes clear that the vaporization rate is directly proportional to the equilibrium vapor pressures. These calculations are fairly accurate. Block-Bolten and Eagar calculated the vaporization rates of different elements using the Langmuir equation during GTA welding of aluminum alloys and were able to correctly predict the evaporation rate of the dominant metal vapors on weld pools.[13] The vaporization rates for the relevant elements for Inconel 718 and Ti-6Al-4V are presented in Figure 14. The partial pressures for the calculations were obtained from the plots by Honig.[14] It can be seen that at 2273 K (2000 °C) the vaporization rate of Cr is nearly six times that of Ni, whereas at 2773 K (2500 °C) it is about twice that of Ni. As a result, larger amounts of Cr are evaporated from the melt pool and that is reflected as an increase in Cr-to-Ni ratio on the heat shield as compared to that in the powder particles. The differences between the vaporization rates are more pronounced in the case of Ti-6Al-4V, where at all temperatures the vaporization rate of Al is at least two to three orders of magnitude larger than the vaporization rates of Ti and V. On the other hand, Ti vaporizes at a faster rate than V at lower temperatures, while at 2773 K (2500 °C) the vaporization rates for both the elements are similar. The manifestation of this can directly be seen from the plots in Figure 13(b). The ratio of Al:Ti in the metallized layer is about five times more than that in the powder particles, thereby causing the metallized layer to be significantly richer in Al. The ratio of V:Ti slightly decreases or stays about the same. However, it is to be noted that the process of melting in the EBM chamber is a continuous one and the elements keep vaporizing as the melt pool cools down from the peak temperature to a solid state. Thus, the ratios predicted by the model cannot be directly used to determine the composition of the metallized layer unless a time-dependent equation is used. Current studies are underway to model the temperature profiles in a melt pool during the melting process, which can then be used to calculate the actual vaporization rates since the vapor pressures are extremely sensitive to temperature.

IV. CONCLUSIONS

1. Inconel 718 powders can sustain a large number of cycles without a change in powder and subsequently build chemistries.
2. Ti-6Al-4V powders are prone to pick up oxygen with increasing number of build cycles. Their use is thus limited by amount of oxygen pickup which reflects in the final builds. The oxygen concentration of the builds steadily increased from 0.141 to 0.168 wt pct.
3. There is no significant change in the flowability, morphology, and size distributions of both Inconel 718 and Ti-6Al-4V powders as a function of build cycles, thus allowing them to be reused over a large number of cycles.
4. Metallization is observed during the processing of both Inconel 718 and Ti-6Al-4V builds with the

metallized layer being rich in Cr for Inconel 718 powders and having a $TiAl_3$ composition for Ti-6Al-4V powders. It is likely that the Cr enrichment on the smooth side of metallized layers is due to the inter-diffusion between the SS-304 heat shield and the metallized products.

Based on the above-mentioned points, it is clear that the initial powder chemistries and the alloy system under consideration are the key factors in governing the recyclability of powders in powder bed systems. Metallization has been observed in both the systems with the similarities being the possible formation mechanism of the particles in the condensed matrix phase along with diffusion across the heat shield and the metallized product, and studies are currently underway to understand the phenomena in detail. Both the alloys can be recycled over a large number of cycles with oxygen pickup being the limiting factor.

ACKNOWLEDGMENTS

Research was sponsored the U.S. Department of Energy, Office of Energy Efficiency and Renewable Energy, Advanced Manufacturing Office, under contract DE-AC05-00OR22725 with UT-Battelle, LLC. This research at the Oak Ridge National Laboratory's High Temperature Materials Laboratory was sponsored by the U.S. Department of Energy, Office of Energy Efficiency and Renewable Energy, Vehicle Technologies Program.

REFERENCES

1. A.A. Antonysamy, J. Meyer, and P.B. Prangnell: *Mater. Charact.*, 2013, vol. 84, p. 153.
2. L.E. Murr, S.M. Gaytan, D.A. Ramirez, E. Martinez, J. Hernandez, K.N. Amato, P.W. Shindo, F.R. Medina, and R.B. Wicker: *J. Mater. Sci. Technol.*, 2012, vol. 28, p. 1.
3. Z. Wang, K. Guan, M. Gao, X. Li, X. Chen, and X. Zeng: *J. Alloy. Compd.*, 2012, vol. 513, p. 18.
4. S.S. Al-Bermani, M.L. Blackmore, W. Zhang, and I. Todd: *Metal. Mater. Trans. A*, 2010, vol. 41A, p. 3422.
5. R.R. Dehoff, M.M. Kirka, W.J. Sames, H. Bilheux, A.S. Tremsin, L.E. Lowe, and S.S. Babu: *Mater. Sci. Technol.*, 2015, vol. 000, p. 1.
6. H.P. Tang, M. Qian, N. Liu, X.Z. Zhang, G.Y. Yang, and J. Wang: *J. Mater. Sci.*, 2015, vol. 67, p. 555.
7. M. Ruffo, C. Tuck, and R. Hague: *Proc. Inst. Mech. Eng. B: J. Eng. Manuf.*, 2006, vol. 220, p. 1417.
8. ASTM B213-13: *Standard Test Methods for Flow Rate of Metal Powders Using the Hall Flowmeter Funnel*, ASTM International, West Conshohocken, PA, 2013.
9. F. Medina: Arcam AB, unpublished research.
10. ASTM F2924-14: *Standard Specification for Additive Manufacturing Titanium-6 Aluminum-4 Vanadium with Powder Bed Fusion*, ASTM International, West Conshohocken, PA, 2013.
11. T.R. Muth, Y. Yamamoto, D.A. Frederick, C.I. Contescu, W. Chen, Y.C. Lim, W.H. Peter, and Z. Feng: *J. Mater. Sci.*, 2013, vol. 65, p. 643.
12. H. Zhao, D.R. White, and T. DebRoy: *Int. Mater. Rev.*, 1999, vol. 44, p. 238.
13. A. Block-Bolten and T.W. Eagar: *Metall. Trans. B*, 1984, vol. 15B, p. 461.
14. R.E. Honig: *RCA Rev.*, 1962, vol. 23, p. 567.